Earth Surface Mineral dust source InvesTigation (EMIT)

EMIT L2b Algorithm: Mineral Detection and Related Products at the Pixel Scale

Theoretical Basis

Philip G. Brodrick, Jet Propulsion Laboratory, Pasadena, CA
Roger N. Clark, Planetary Science Institute, Tucson AZ
Gregg A. Swayze, U. S. Geological Survey, Denver, CO
Raymond Kokaly, U. S. Geological Survey, Denver, CO
John Meyer, U.S. Geological Survey, Denver CO
Bethany Ehlman, California Institute of Technology, Pasadena, CA
Abigail Keebler, California Institute of Technology, Pasadena, CA
David R. Thompson, Jet Propulsion Laboratory, Pasadena, CA
Robert O. Green, Jet Propulsion Laboratory, Pasadena, CA

Version 1.0

May 2023

Jet Propulsion Laboratory
California Institute of Technology
Pasadena, California 91109-8099

Change Log

Version	Date	Comments
0.1	Sept, 2019	Initial Draft
0.2	March 2020	Refinement for demo SDS
0.3	May 2023	First Release of L2BMIN

Table of Contents

Disclaimer

The EMIT L2b approach was developed to support the EMIT mission objectives of constraining the sign of dust related radiative forcing. Ten mineral types are the core focus of this work: Calcite, Chlorite, Dolomite, Goethite, Gypsum, Hematite, Illite+Muscovite, Kaolinite, Montmorillonite, and Vermiculite. Additional minerals are included in the L2BMIN product for transparency and completeness, but were not the focus of this effort. Further validation is required to use these additional mineral maps – particular in the case of resource exploration. Similarly, the separation of minerals with similar spectral features - say a fine-grained goethite and hematite - is an area of active research. The results presented here are an initial offering, but the precise categorization is likely to evolve over time, and the limits of what can and cannot be separated on the global scale is still being explored. The user is encouraged to read the ATBD for more details.

1. Key Team Members

A large number of individuals contributed to the development of the algorithms, methods, and implementation of the L2b approach for EMIT. The primary contributors are the following:

- Philip G. Brodrick (Jet Propulsion Laboratory)
- Roger N. Clark (Planetary Science Institute)
- Gregg A. Swayze (U.S. Geological Survey)
- Raymond Kokaly (U.S. Geological Survey)
- John Meyer (U.S. Geological Survey)
- Bethany Ehlman (California Institute of Technology)
- Abigail Keebler (California Institute of Technology)
- David R. Thompson (Jet Propulsion Laboratory)

2. Historical Context and Background on the EMIT Mission and its Instrumentation

Mineral dust aerosols originate as soil particles lifted into the atmosphere by wind erosion. Mineral dust created by human activity makes a large contribution to the uncertainty of direct radiative forcing (RF) by anthropogenic aerosols (USGCRP and IPCC). Mineral dust is a prominent aerosol constituent around the globe. However, we have poor understanding of its direct radiative effect, partly due to uncertainties in the dust mineral composition. Dust radiative forcing is highly dependent on its mineral-specific absorption properties. The current range of iron oxide abundance in dust source models translates into a large range of values, even changing the sign of the forcing (-0.15 to 0.21 W/m2) predicted by Earth System Models (ESMs) (Li et al., 2020). The National Aeronautics and Space Administration (NASA) recently selected the Earth Surface Mineral Dust Source Investigation (EMIT) to close this knowledge gap. EMIT will launch an instrument to the International Space Station (ISS) to directly measure and map the soil mineral composition of critical dust-forming regions worldwide.

The EMIT Mission will use imaging spectroscopy across the visible shortwave (VSWIR) range to reveal distinctive mineral signatures, enabling rigorous mineral detection, quantification, and mapping. The overall investigation aims to achieve two objectives:

1. Constrain the sign and magnitude of dust-related RF at regional and global scales. EMIT achieves this objective by acquiring, validating and delivering updates of surface mineralogy used to initialize ESMs,
2. Predict the increase or decrease of available dust sources under future climate scenarios. EMIT achieves this objective by initializing ESM forecast models with the mineralogy of soils exposed within at-risk lands bordering arid dust source regions.

The EMIT instrument is a Dyson imaging spectrometer that will resolve the distinct spectral absorptions of iron oxides, clays, sulfates, carbonates, and other dust-forming minerals with contiguous spectroscopic measurements in the visible to short wavelength infrared region of the spectrum. EMIT will map mineralogy with a spatial sampling to detect minerals at the one hectare scale and coarser, ensuring accurate characterization of the mineralogy at the grid scale required by ESMs. EMIT's fine spatial sampling will resolve the soil exposed within hectare-scale agricultural plots and open lands of bordering arid regions, critical to understanding feedbacks caused by mineral dust arising from future changes in land use, land cover, precipitation, and regional climate forcing.

The EMIT Project is part of the Earth Venture-Instrument (EV-I) Program directed by the Program Director of the NASA Earth Science Division (ESD). EMIT is comprised of a VSWIR Infrared Dyson imaging spectrometer adapted for installation on the International Space Station (ISS).

Table 1 below describes the different data products the EMIT Mission will provide to the data archives. This document describes the "Level 2b" stage which relies on outputs from the Level 2A algorithms (cloud masking, standing water, vegetation cover) and the Level 2B mineral detection algorithms to produce mineral maps that can be aggregated (L3) and assimilated into Earth System models to evaluate Radiative Forcing (RF) impacts (Level 4).

Table 1. Emit Data Product Hierarchy

Data Product	Description	Initial Availability	Median Latency Post-delivery	NASA DAAC
Level 0	Raw collected telemetry.	4 months after IOC	2 months	LP DAAC
Level 1a	Reconstructed, depacketized, uncompressed data, time referenced, annotated with ancillary information reassembled into scenes.	4 months after IOC	2 months	LP DAAC
Level 1b	Level 1a data processed to sensor units including geolocation and observation geometry information.	4 months after IOC	2 months	LP DAAC
Level 2a	Surface reflectance derived by screening clouds and correction for atmospheric effects.	8 months after IOC	2 months	LP DAAC
Level 2b	Mineralogy derived from fitting reflectance spectra, screening for non-mineralogical components.	8 months after IOC	2 months	LP DAAC
Level 3	Gridded map of mineral composition aggregated from Level 2b with uncertainties and quality flags.	11 months after IOC	2 months	LP DAAC

Level 4	Earth System Model runs to address science objectives	16 months after IOC	2 months	LP DAAC

The Level 2b step can be loosely summarized through Error! Reference source not found., whereby measured reflectance as reported by Level 2a is used in combination with a spectral library and a series of mineral detection algorithms to produce mineral distribution maps. This process is broken into two steps: an identification and band depth estimation, and then an aggregation to spectral abundance of 10 key minerals for Earth System Models. Significant additional details are discussed in Section 4. A high-level, yet complete, workflow of the EMIT science data system is shown in Figure 1 for context.

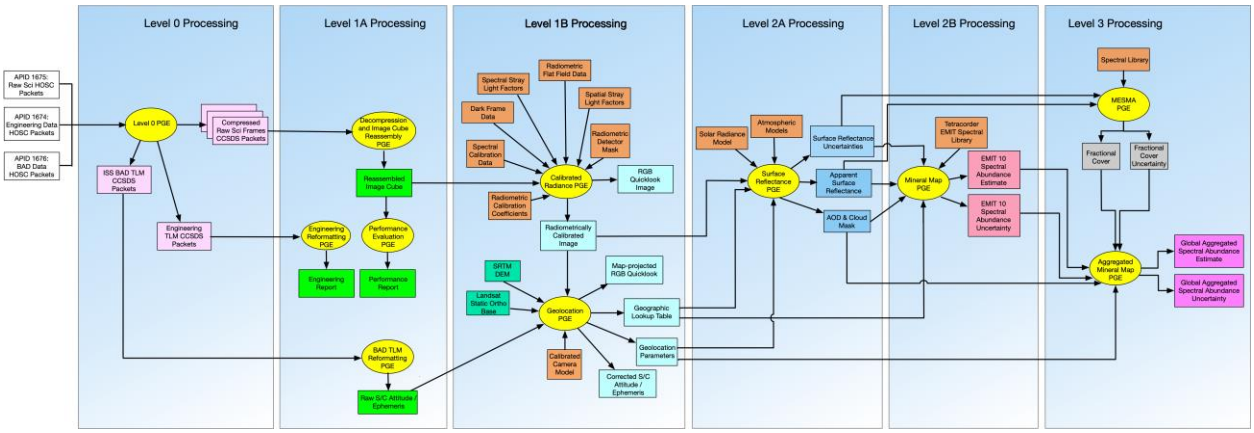

Figure 1. **High-level workflow of the EMIT science data system.**

3. Algorithm Rationale

The EMIT L2b approach builds on a substantial history of mineral identification with airborne imaging spectrometers. We leverage the Tetracorder system (Clark et al., 2003), which has been developed for over 30 years by spectroscopists at the U.S. Geological Survey and the Planetary Science Institute, along with additional collaborators. The Tetracorder mineral identification approach has been validated at numerous desert sites throughout the Southwestern U.S. (Clark et al., 2003; Swayze 1997; Swayze et al., 2014) using the Airborne Visible Infrared Imaging Spectrometer (AVIRIS-C, Green et al., 1998). Tetracorder has also been shown to be effective in a wide variety of environmental investigations (e.g. Swayze et al., 2000, 2009, 2014; Clark et al., 2001, 2006; Livo et al., 2007), demonstrating the general applicability of the approach.

4. Algorithm Description

4.1 Input data

EMIT output data products delivered to the DAAC use a netCDF-4 standard, but the system operates internally on data products stored as binary data cubes with detached human-readable ASCII header files. The precise formatting convention adheres to the ENVI standard, accessible (Jan 2020) at https://www.harrisgeospatial.com/docs/ENVIHeaderFiles.html. The header files all consist of data fields in equals-sign-separated pairs, and describe the layout of the file. In the file descriptions below, *n* denotes the number of lines particular to the given acquisition.

The specific input files needed for the L2b stage are:

1. **Surface reflectance,** provided as an *n* x 1242 x *c* BIL interleave data cube, where each of *c* channels corresponds to a different wavelength.
2. **Channelized surface reflectance uncertainty,** provided as an *n* x 1242 x *c* BIL interleave data cube, where each of *c* channels corresponds to a different wavelength.

4.2 Theoretical description

The goal of the Level 2b as a whole is to quantify surface minerology based on surface reflectance. Surface mineral detection relies on the distinct spectral signatures over the 380-2500 nm spectral region, as demonstrated for the EMIT-10 minerals in Figure 2. Mapping these minerals requires *in situ* knowledge of the spectral reflectance of minerals as well as a system to match that *in situ* knowledge to remotely-sensed surface reflectance in a manner that minimizes the risk of misidentification.

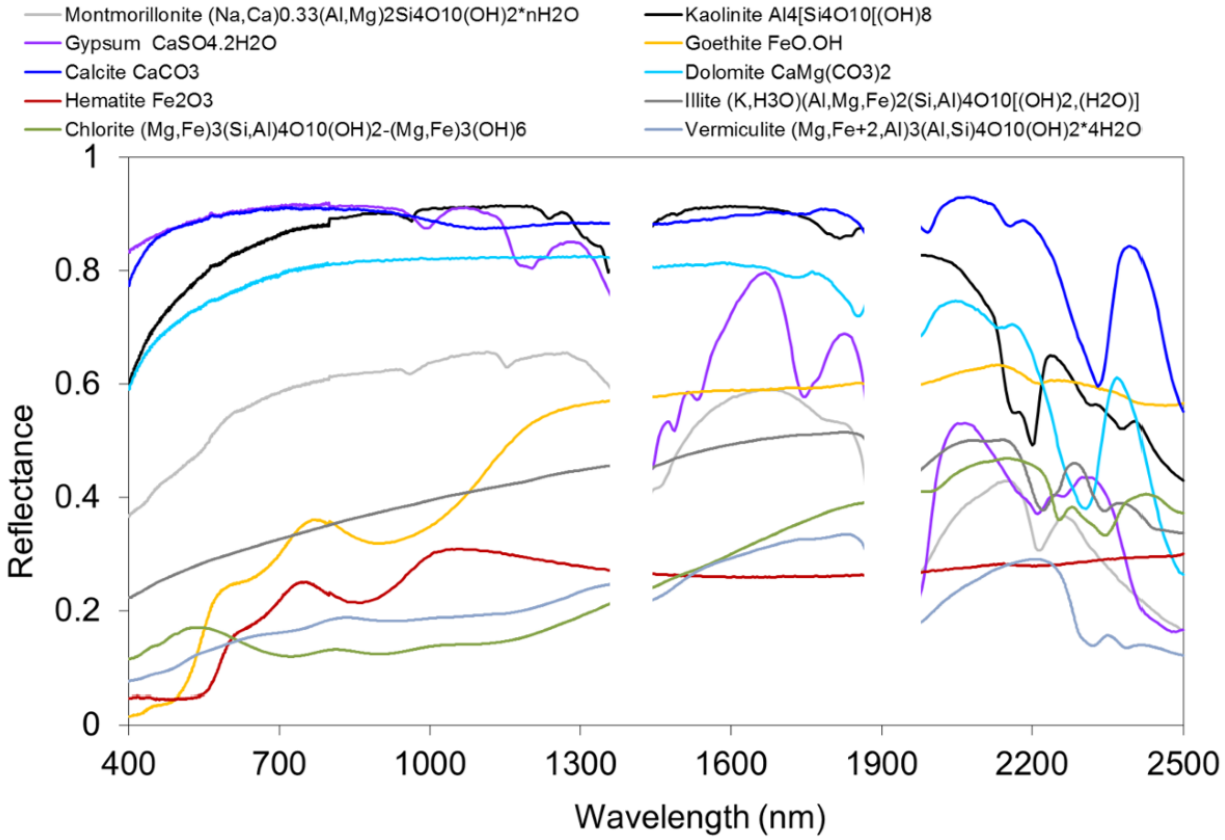

Figure 2. Reflectance spectra in the VSWIR spectral region for the designated EMIT dust source minerals. These spectra demonstrate distinct spectral signatures in specific regions, which facilitates mapping mineral composition.

Level 2b outputs are generated in two steps. First, the strength of the spectral signature of a wide range of surface constituents is determined by feature matching L2a surface reflectance with spectra of reference minerals selected from the USGS Spectral Library 06 (Clark et al. 2007), augmented with a research library, using the Tetracorder system (Clark et al., 2003; see Section 4.2.1). Next, the strengths of the spectral signatures of key reference constituents are aggregated to estimate the spectral abundance of each of the EMIT 10 minerals (Section 4.2.2). Each of these two steps has an independent data product, in order to maximize the transparency and utility of the retrievals.

4.2.1 Surface constituent mapping

Surface material mapping is performed using linear feature matching through the Tetracorder system, and ultimately generates independent maps for each reference library constituent. Surface materials include not only pure components, but also mixtures of components (e.g., multiple minerals in areal, intimate, and molecular mixtures, coatings, minerals and plant combinations, etc.). While the spectral identification process is documented in detail in Clark et al. (2003), in brief, it occurs by matching absorption features of predefined spectral regions to selected spectra from a reference library convolved to the EMIT spectrometer's spectral resolution. Spectral features for the EMIT mission will come from the Tetracorder 5.27 command file cmd.lib.setup.t5.27d1. For each pixel *i*, all remotely sensed spectra are continuum-normalized for each spectral feature *j* as

$$O_j^i(w) = 1 - \frac{R(w)}{R_c(w)}, \tag{1}$$

$$L_j(w) = 1 - \frac{S(w)}{S_c(w)}, \tag{2}$$

where R is the observed apparent surface reflectance input from L2a, S is the library reference spectrum, the subscript c indicates the continuum reflectance linearly interpolated between two preselected continuum endpoints of the spectral feature of interest, and O and L are the continuum-normalized observed and library spectra respectively. O, C, S, L, and R are functions of wavelength (w). Corresponding continuum-normalized values for the library reference materials, L_j, are also calculated. As described in Clark et al. (2003), on a per-pixel basis, L_j is scaled by a constant linear factor a_j^i and offset by a second linear factor b_j^i to best match O_j^i over the full spectral feature, as

$$a_j^i = \text{argmin} \sum_{w \in W} \left(\left(a_j^i \, L_j^i(w) + b_j^i \right) - O_j^i(w) \right)^2 \tag{3}$$

$$= \frac{n \sum_{w \in W} O_j^i(w) L_j(w) - \sum_{w \in W} O_j^i(w) \sum_{w \in W} L_j(w)}{n \sum_{w \in W} L_j^2(w) - \left(\sum_{w \in W} L_j(w) \right)^2} \tag{4}$$

And at this point, the band depth – a measure of the strength of the identified absorption feature - can be calculated as:

$$B_j^i(w) = L(w_j^*) \; a_j^i, \tag{5}$$

where

$$w_j^* = \text{argmax} \, L_j(w). \tag{6}$$

The quality of the feature match between continuum-removed (and scaled) spectra for constituent *j* is then calculated as the correlation coefficient *F*, adapted from Clark et al. (2003) as:

$$F_j = \frac{n\sum_{w\in W} O_j^i(w)L_j(w) - \sum_{w\in W} O_j^i(w)\sum_{w\in W} L_j(w)}{n\sum_{w\in W}\left(L_j^2(w) + {O_j^i}^2(w)\right) - \left(\sum_{w\in W} L_j(w)\right)^2 + \left(\sum_{w\in W} O_j(w)\right)^2} \quad (4)$$

when all sums are calculated over the wavelength interval *W* for the given spectral feature which has *n* channels.

This fit is calculated for all selected reference spectra within a designated spectral region (i.e., a spectral group). The reference spectrum with the best fit is identified as the "observed" material within the given spectral region for the particular EMIT observed spectra. Spectral matches have to meet predetermined requirements, placed on factors such as goodness of fit, depth, the product of depth and fit, reflectance level (brightness), continuum slope, and/or the presence/absence of key ancillary spectral features. Spectral matches that fail to meet these requirements are discarded. Requirements are established in the Tetracorder 5.27 command file cmd.lib.setup.t5.27d1.

The spectral features defined in the Tetracorder command file cmd.lib.setup.t5.27d1 include 23 spectral groups in total, which are reduced to those that are spanned by the wavelengths measured by EMIT, and are shown in Table 2. The dominant mineral detection groups, Groups 1 and 2, are very similar to those in Clark et al. (2003, 2010) and Swayze et al. (2003, 2014), with minor improvements made by subsequent studies and from initial EMIT mapping estimates. These groups should not be confused with geologic groups, though there is some overlap.

Table 2. Tetracorder EMIT Expert System Groups and Cases

Group	Function
Group 0	Catchall for materials common to all other spectral groups
Group 1	Electronic absorptions in the visible and 1-micron regions
Group 2	Narrow absorptions in the 2 to 2.5-micron region (e.g. clays, carbonates, sulfates)
Group 3	Vegetation detection
Group 4	Broad absorptions in the 1.5-micron region
Group 5	Broad absorptions in the 2-micron region
Case 1	Vegetation red edge shift
Case 2	Vegetation spectral type
Case 3	Vegetation water band depth: 0.95-micron band
Case 4	Vegetation water band depth: 1.15-micron band
Case 5	Vegetation water band depth: 1.4-micron band

The identified minerals from Groups 1 and 2, along with the associated band depths, are delivered in the **EMIT L2B Estimated Mineral Identification Band Depth and Uncertainty** product (EMIT_L2B_MIN and EMIT_L2B_MINUNCERT). A mineral grouping matrix is available on the emit-sds-l2b repository (https://github.com/emit-sds/emit-sds-l2b/blob/develop/data/mineral_grouping_matrix_20230503.csv), which documents the library constituents for Groups 1 and 2. In the delivered output file, the mineral ID links to the index column from the given table. The Library column indicates the library source for each constituent ('splib06' for the USGS Spectral Library 06, and 'sprlb06' for research library

constituents that augment the USGS library). The URL column links to a description of each library element from the USGS Spectral Library 07 (descriptions are consistent between library 06 and 07). The exact spectral library used – convolved to the EMIT wavelengths - is also available on Zenodo, both as a SPECPR file and converted into an ENVI binary file.

For simplicity in the delivery, we merge the band depth from each Group 1 mineral together into the same file (there can be one and only one value), and do the same with Group 2 minerals. A separate channel indicates which mineral was detected from each of Group 1 and Group 2, with a 0 indicating no detection and -9999 indicating a lack of available data.

4.2.2 EMIT-10 Aggregation

An updated form of this documentation describing the aggregation step of individual constituent band depths to EMIT-10 mineral spectral abundances will be released soon.

4.3 Practical Considerations

Computation is largely input-output limited, and the calculations are fast relative to L2a. All relevant dependencies, including spectral reference libraries, are available on the official repository. Tetracorder is available open-source at https://github.com/PSI-edu/spectroscopy-tetracorder, and the EMIT SDS has a fork with minor installation changes at https://github.com/emit-sds/spectroscopy-tetracorder.

5. Output Data

Level 2b output data comes in two deliveries. The first, Level l2bmin is described here. L2bmin has both *delivered* both *delivered* products, which are necessary for mission success, as well as *auxiliary* products, which are generated in the process of producing the delivered products, and preserved for transparency and issue tracking.

4.4.1 Delivered Products

1. **EMIT L2B Estimated Mineral Identification and Band Depth 60 m,** provided as *n* x 1280 x 4 BIL interleave data cubes. The first band contains the Group 1 band depth, the second band contains the Group 1 mineral identification, the third band contains the Group 2 band depth, and the fourth band contains the Group 2 mineral identification.
2. **EMIT L2B Estimated Mineral Identification and Band Depth Uncertainty 60 m,** provided as *n* x 1280 x 4 BIL interleave data cubes. The first band contains the Group 1 band depth uncertainty, the second band contains the fit score (R^2) of the mineral match, the third band contains the Group 2 band depth uncertainty, and the fourth band contains the Group 2 fit score (R^2).

4.4.2 Auxiliary Products

1. **Raw tetracorder output,** a tar file of the complete set of tetracorder 5.27d2 configuration scripts and results are preserved.

6. Calibration, uncertainty characterization and propagation, and validation

6.1 Uncertainty quantification

Uncertainty characterization of the L2b products are calculated by propagating wavelength-specific measurement uncertainty forward from the L2a product. For simplicity, we approximate the uncertainty of a continuum removed reflectance feature at a particular wavelength (e.g. $O_j^i(w)$) as the measurement uncertainty of the reflectance spectrum at that same wavelength, which we denote as $\Psi_R(w)$, relying on the assumption that the continuum endmember definitions build no additional uncertainty into the calculation. Given that the reflectance uncertainty estimates are channel-wise independent, we can then estimate the band depth uncertainty as the square root of the partial derivative of the band depth by each wavelength:

$$\Psi_{B_j}^i = \sqrt{\sum_{w \in W} \left(\left| \frac{\delta B_j^i(w)}{\delta L(w)} \right|^2 \Psi_{\mathrm{R}}^2(\mathrm{w}) \right)} \tag{6}$$

$$\Psi_{B_j}^i = \sqrt{\sum_{w \in W} (L(w) c\, n)^2 + \sum_{w \in W} \left(\sum_{w \in W} L(w) \right)^2 \Psi_R^2(w)} \tag{7}$$

where c is the convenience function

$$c = \frac{L(w^*)}{n \sum_{w \in W} L(w)^2 - \left(\sum_{w \in W} L(w) \right)^2} \tag{8}$$

where $\Psi_{B_j}^i$ is the band depth uncertainty of a given constituent in a given pixel.

While $\Psi_{B_j}^i$ represents a reasonable estimation of the propagated surface reflectance uncertainty, several additional sources of potential error are not considered here. Most notably, this includes any misidentification of minerals within the spectral library, which would not be captured. The fit score (Equation 4), which is also provided, gives a measure of the strength of the match between the observed and library spectra, but also does not fully capture misidentification. With imaging spectroscopy measurements being taken for many regions of the planet for the first time, it is likely that spectra of additional materials will need to be added to the reference library in order to better characterize the surface. This is consistent with previous use of the Tetracorder system, though the need for augmentation of spectral libraries used in studies with Tetracorder have decreased over time. A significant round of spectral reference library augmentations were made circa 2010 to incorporate organics and man-made materials found in urban environments (Clark et al., 2010; Kramer et al., 2010; Pieters et al., 2010; Swayze et al., 2009), and since then newer studies have introduced significantly fewer changes (e.g. Swayze et al. (2014)), as compared to earlier studies.

6.2 Validation at Known Sites

The Tetracorder mineral identification approach has been previously validated at numerous desert sites throughout the Southwestern U.S. (Clark et al., 2003 and Swayze et al., 2014), based primarily on laboratory electron probe microanalysis, petrographic, SEM, spectroscopic, and X-ray diffraction measurements of samples collected from areas spectrally dominated by one or more VSWIR active minerals including those on the EMIT list.

Validation of EMIT specific Tetracorder products can be accomplished by comparison of EMIT L2b products with those equivalently derived from AVIRIS data. Relevant regions with extensive coverage that have been relatively well (mineralogically) characterized, and which have significant enough coverage so as to likely be included in EMIT coverage, include those shown in Table 3.

Validation activities for EMIT are ongoing, and this document will be updated in the future to reflect those efforts.

Table 3. EMIT mineral mapping validation sites and their minerals.

Mineral Validation Site	Spectrally Dominant Mineralogy
Arches National Park, Utah	Calcite, dolomite, goethite, gypsum, hematite, illite, kaolinite, montmorillonite
Cuprite, Nevada	Calcite, chlorite, goethite, hematite, illite, kaolinite, calcite, montmorillonite
Mountain Pass, California	Dolomite, vermiculite
Salton Sea area, California	Carbonates, goethite, hematite, kaolinite
White Sands, New Mexico	Gypsum

7. Constraints and Limitations

No constraints or limitations are imposed on the L2b products. All delivered data will have undergone quality control and should be considered valid, calibrated data up to the reported uncertainties in input parameters. Unanticipated data corruption due to factors outside the modeling, if discovered, will be reported in peer reviewed literature and/or addenda to this ATBD.

8. Code Repository and References

Code for L2B can be found at https://github.com/emit-sds/emit-sds-l2b, with support of other repositories at https://github.com/emit-sds/. Code for Tetracorder is available at https://github.com/PSI-edu/spectroscopy-tetracorder, with a fork for the exact implementation used by the EMIT SDS (mostly installation changes) available at https://github.com/emit-sds/spectroscopy-tetracorder.

References

Clark, R. N., R. O. Green, G. A. Swayze, G. Meeker, S. Sutley, T. M. Hoefen, K. E. Livo, G. Plumlee, B. Pavri, C. Sarture, S. Wilson, P. Hageman, P. Lamothe, J. S. Vance, J. Boardman I. Brownfield, C. Gent, L. C. Morath, J. Taggart, P. M. Theodorakos, and M. Adams, 2001, Environmental Studies of the World Trade Center area after the September 11, 2001 attack. U. S. Geological Survey, *Open File Report OFR-01-0429*, (approximately 260 pages printed), 2001. http://pubs.usgs.gov/of/2001/ofr-01-0429/

Clark, R.N., Swayze, G.A., Livo, K.E., Kokaly, R.F., Sutley, S.J., Dalton, J.B., McDougal, R.R., and Gent, C.A. 2003. Imaging spectroscopy: Earth and planetary remote sensing with the USGS Tetracorder and expert systems, *Journal of Geophysical Research*, Vol. 108(E12), 5131, doi:10.1029/2002JE001847, p. 5-1 to 5-44.
http://speclab.cr.usgs.gov/PAPERS/tetracorder

Clark, R.N., G.A. Swayze, T.M. Hoefen, R.O. Green, K.E. Livo, G., Meeker, S. Sutley, G. Plumlee, B. Pavri, C. Sarture, J. Boardman, I., Brownfield, L.C. Morath, 2006, Chapter 4: Environmental mapping of the World Trade Center area with imaging spectroscopy after the September 11, 2001 attack: in *Urban Aerosols and Their Impacts: Lessons Learned from the World Trade Center Tragedy*, Jeff Gaffney and N. A. Marley (eds), *American Chemical Society*, Symposium Series 919, Oxford University Press, p. 66-83, plates 4.1-4.6. http://www.us.oup.com/us/catalog/general/subject/Chemistry/EnvironmentalChemistry/?view=usa&ci=9780841239166

Clark, R.N., Swayze, G.A., Wise, R., Livo, E., Hoefen, T., Kokaly, R., Sutley, S.J., 2007, USGS digital spectral library splib06a: *U.S. Geological Survey Data Series 231*, http://speclab.cr.usgs.gov/spectral-lib.html with over 6000 web pages, and data files.

Clark, R.N., Swayze, G.A., Leifer, I. Livo, K.E., Kokaly, R., Hoefen, T., Lundeen, S., Eastwood, M., Green, R.O., Pearson, N., Sarture, C., McCubbin, I., Roberts, D., Bradley, E., Steele, D., Ryan, T., Dominguez, R., and the Air borne Visible/Infrared Imaging Spectrometer (AVIRIS) Team, 2010, A method for quantitative mapping of thick oil spills using imaging spectroscopy: *U.S. Geological Survey Open-File Report 20101167*, 51 p. http://pubs.usgs.gov/of/2010/1167/

Green, R.O., Eastwood, M.L., Sarture, C.M., Chrien, T.G., Aronsson, M., Chippendale, B.J., Faust, J.A., Pavri, B.E., Chovit, C.J., Solis, J., Olah, M.R., Williams, O., 1998, Imaging spectroscopy and the Airborne Visible/Infrared Imaging Spectrometer (AVIRIS): *Remote Sensing of Environment*, v. 65, p. 227-248.

Kokaly, R.F., R. N. Clark, G. A. Swayze, K. E. Livo, T. M. Hoefen, N. C. Pearson, R. A. Wise, W. M. Benzel, H. A. Lowers, R. L. Driscoll, and A. J. Klein, 2017, USGS Spectral Library Version 7: U.S. Geological Survey Data Series 1035, 61 p., https://doi.org/10.3133/ds1035. https://speclab.cr.usgs.gov/spectral-lib.html

Kramer, Georgiana Y., Sebastien Besse, Jeffrey Nettles, Jean-Philippe Combe, Roger N. Clark, Carle M. Pieters, Matthew Staid, Erik Malaret, Joseph Boardman, Robert O. Green, Thomas B. McCord, James W. Head III, 2010, Newer Views of the Moon: Comparing Spectra from 1 Clementine and the Moon Mineralogy Mapper, *J. of Geophysical Research* **116**, E00G04, doi:10.1029/2010JE003728.

Li, L., Mahowald, N., Balkanski, Y., Connelly, D., Ginoux, P., Ageitos, M. G., Hamilton, D., Kalashnikova, O., Klose, M., Miller, R. L., Obiso, V., Paynter, D. and Perez Garcia-Pando, C.: Large contribution of hematite and geothite to uncertainty in dust direct radiative forcing, Atmos. Chem. Phys., 2020.

Livo, K.E., Kruse, F.A., Clark, R.N., Kokaly, R.F., and Shanks, W.C. III, 2007, Hydrothermally Altered Rock and Hot- Spring Deposits at Yellowstone National Park—Characterized Using Airborne Visible- and Infrared-Spectroscopy Data, Chapter O in: Integrated Geoscience Studies in the Greater Yellowstone Area—Volcanic, Tectonic, and Hydrothermal Processes

in the Yellowstone Geoecosystem, *USGS Professional Paper 1717*, 463-489.

Pieters, C. M., J. N. Goswami, R. N. Clark, M. Annadurai, J. Boardman, B. Buratti, J.-P. Combe, M. D. Dyar, R. Green, J. W. Head, C. Hibbitts, M. Hicks, P. Isaacson, R. Klima, G. Kramer, S. Kumar, E. Livo, S. Lundeen, E. Malaret, T. McCord, J. Mustard, J. Nettles, N. Petro, C. Runyon, M. Staid, J. Sunshine, L. A. Taylor, S. Tompkins, P. Varanasi, 2009, Character and Spatial Distribution of OH/H_2O on the Surface of the Moon seen by M3 on Chandrayaan-1 *Science*, **326**, 568-572, DOI: 10.1126/science.1178658.

Swayze, G. A., 1997, The hydrothermal and structural history of the Cuprite mining district, southwestern Nevada: An integrated geological and geophysical approach, Ph.D. thesis, 399 pp., Univ. of Colorado, Boulder, Colo.

Swayze, G.A., K.S. Smith, R.N. Clark, S.J. Sutley, R.N. Pearson, G.S. Rust, J.S. Vance, P.L. Hageman, P.H. Briggs, A.L. Meier, M.J. Singleton, and S. Roth, 2000, Using imaging spectroscopy to map acidic mine waste, *Environmental Science and Technology*, **34**. 47-54.

Swayze, G.A., Kokaly, R.F., Higgins, C.T., Clinkenbeard, J.P., Clark, R.N., Lowers, H.A., and Sutley, S.J., 2009, Mapping potentially asbestos-bearing rocks using imaging spectroscopy: *Geology*, **37**, 763-766.

Swayze, G.A., Clark, R.N., Goetz, F.H., Chrien, T.G., and Gorelick, N.S., 2003, Effects of spectrometer band pass, sampling, and signal-to-noise ratio on spectral identification using the Tetracorder algorithm: *Journal of Geophysical Research* (Planets), **108**, 5105, doi: 10.1029/2002JE001975, 30 p.

Swayze, G.A., Clark, R.N., Goetz, A.F.H, Livo, K.E., Breit, G.N., Sutley, S.J., Kruse, F.A., Snee, L.W., Lowers, H.A., Post, J.L., Stoffregen, R.E., and Ashley, R.P., 2014, Mapping advanced argillic alteration at Cuprite, Nevada using imaging spectroscopy: *Economic Geology*, **109**, 1179-1221 DOI: 10.2113/econgeo.109.5.1179